Eur. Phys. J. B **58**, 115–121 (2007)
DOI: 10.1140/epjb/e2007-00218-0

THE EUROPEAN PHYSICAL JOURNAL B

# Effect of $Ta^{5+}$ substitution for Mn on the ground state of $La_{0.67}Ca_{0.33}MnO_3$

L. Seetha Lakshmi[1,2,a], K. Dörr[2], K. Nenkov[2], A. Handstein[2], V.S. Sastry[1], and K.-H. Müller[2]

[1] XS & CGS, Materials Science Division, Indira Gandhi Centre For Atomic Research, Kalpakkam, 603102, Tamil Nadu, India
[2] Institute of Metallic Materials, IFW Dresden, Postfach 270116, Dresden 01171, Germany

Received 12 April 2007 / Received in final form 28 June 2007
Published online 10 August 2007 – 

**Abstract.** We report the charge state modification effects at the Mn site on the ground state properties of colossal magnetoresistive manganites. $Ta^{5+}$ substitution results in an appreciable increase in the lattice parameters and unit cell volume due to increased $Mn^{3+}$ concentration. The ferromagnetic-metallic ground state modifies to a cluster glass insulator for $x \geqslant 0.05$. The reduction in the transition temperatures with increasing $x$ is ∼39 K/at.%. Besides the modification of majority carrier concentration due to increased $Mn^{3+}$ concentration and enhanced local structural effects, the local electrostatic potential of the substituent seems to contribute to the unusually strong reduction of the transition temperatures of the compounds. Thermo magnetic irreversibility just below Curie temperature ($T_c$), non-saturation of magnetization, two distinct magnetic transitions in ac susceptibility in an appropriate static field: close to $T_c$ and other at low temperature (the spin freezing temperature ($T_g$)) and non-stationary dynamics with a characteristic maximum in the magnetic viscosity close to $T_g$ confirm a cluster glass state for $x \geqslant 0.05$. These results find additional support from a linear low temperature magnetic specific heat of $x = 0.10$ with a characteristic broad maximum close to $T_g$.

**PACS.** 75.47.Lx Manganites – 75.50.Lk Spin glasses and other random magnets – 75.40.Cx Static properties – 75.40.Gb Dynamic properties

## 1 Introduction

Enormous efforts on the theoretical and experimental fronts have converged on the idea that manganites are intrinsically inhomogeneous at various length scales [1,2] and the strong interplay between charge, spin, lattice and orbital degrees of freedom leads to a variety of phases with distinct ground state properties [3,4]. Further, it has been argued that stability of ferromagnetic-metallic phase and the occurrence of glassy ground states are affected by competing magnetic interactions in the background of quenched disorder [5,6]. Hence, the studies addressing the disorder effects are of current interest and experimentally it can be achieved by suitable substitutions at the La and / or Mn site. Moreover, the phase-segregated state with glassy characteristics [7] challenges the current understanding of the system and many more exciting results are expected in the near future.

Extensive studies on the La site substitutions established the fact that not only the carrier density ($n$), average ionic size of the La site ($\langle r_A \rangle$) or tolerance factor $t$ [8–10], but also A-site disorder ($\sigma^2$)effect, as suggested by Rodriguez-Martínez et al. [11], plays an important role in controlling the ground state properties of the compounds. Recently, Williams et al. [12] have explored the significance of yet another parameter, namely, the charge disorder effects $\left(\sigma^2\left(q_A\right)\right)$ on the physical properties of rare-earth substituted manganites. Their study demonstrates that the effect of random electrostatic potential due to the differences in the formal charge between La site substituted ions have no significant effect on the transition temperatures [12, 13]. On the contrary, charge state modification at the Mn site, that forms the basis of the present study, is found to have dramatic effect on the physical properties of the CMR manganites.

As the essential degrees of freedom are intimately linked to Mn ion, Mn site substitution offers a direct probe to elucidate its physical properties. Earlier works show that all the substituents in ferromagnetic metallic manganites, irrespective of their chemical nature lower the ferromagnetic transition temperature, but to different extents [14–18] and eventually lead to insulating states exhibiting glassy phases for still higher concentration of the substitutions. In our previous studies on Mn site substitutions with both diamagnetic and paramagnetic ions, we rationalized the variation of extent of suppression in the transition temperatures with concentration ($dT_c/dx$) in terms of local structural modification due to size mismatch and local magnetic coupling between the magnetic moments of substituents and Mn ion [19].

[a] e-mail: slaxmi73@gmail.com

In this paper, we address the significance of yet another important contribution, namely, the charge state modification effects at the Mn site on its physical properties. With this notion, we report the effect of pentavalent Ta substitution at the Mn site of $La_{0.67}Ca_{0.33}MnO_3$: Diamagnetic ($4d^{10}$) $Ta^{5+}$ ion having its ionic radius (0.640 Å) very close to that of $Mn^{3+}$ ion (0.645 Å) [20]. Also by virtue of its closed shell configuration, $Ta^{5+}$ ion does not introduce any additional magnetic coupling effects. As will be shown subsequently, pentavalent Ta beyond 3 at.% substitution modifies the ferromagnetic-metallic ground state of $La_{0.67}Ca_{0.33}MnO_3$ compounds. Modification of the magnetic ground state is inferred from additional features of in the in-phase component of ac susceptibility ($\chi'(T)$), viz., presence of a cusp-like anomaly just below Curie temperature ($T_c$) and a broad shoulder in $\chi'$ at lower temperatures. These compounds are further characterized using static field biased and frequency dependent ac susceptibility. Using static field biased ac susceptibility, the two possible magnetic transitions, viz., paramagnetic to ferromagnetic transition, intra-cluster in nature and the glass transition at lower temperatures are identified. Furthermore, the dynamics of spin freezing probed using the frequency dependent ac susceptibility in the presence of static bias field confirms the glassy ground state of the compounds. The static response of the system is examined using field dependent dc thermo-magnetization under ZFC and FC condition and field dependent magnetization at selected temperatures. These studies indicate the cluster-glass state of the compounds. These results find additional support from the relaxation measurements and the specific heat studies under zero field carried out for $x = 0.10$, the highest substitution level of this study. The detailed analysis of the thermoremanent magnetization and specific heat of the compounds is being published elsewhere [21]. From the inter comparison of the structural, transport and the magnetic properties of the compounds, we propose that the charge state modification effects at the Mn site are most detrimental to the ferromagnetic-metallic ground state of colossal magnetoresistive manganites.

## 2 Experiment

Polycrystalline $La_{0.67}Ca_{0.33}Mn_{1-x}Ta_xO_3$ ($0 \leqslant x \leqslant 0.10$) compounds were synthesized by solid state reaction according to the procedure described in detail elsewhere [22]. The final sintering of the samples at 1525 °C for 24 h was carried out in a single batch to ensure identical sintering conditions. The high statistics room temperature powder X-ray diffraction (XRD) patterns in Bragg-Brentano parafocusing geometry were recorded in the $2\theta$ range, 15–120° with a step size of 0.05°, using $Cu_{K\alpha}$ radiation (STOE, Germany). The structural parameters were estimated using GSAS Rietveld refinement program [23] and SPUDS program [24] to generate the starting model for the Rietveld analysis.

The temperature variation of resistivity ($\rho(T)$) was measured by conventional four probe method. A spilt coil superconducting magnet was employed for steady magnetic fields up to 7 T with magnetic field parallel to the current. The temperature variation of ac susceptibility ($\chi'(T)$) under an ac probe field ($h$) of 1 Oe and an excitation frequency $f$ of 133 Hz was measured using a Lakeshore 7000 series susceptometer. The frequency and static field biased $\chi'(T)$ was carried out in zero field condition using a physical property measurement system (PPMS- Quantum Design). ZFC and field cooled (FC) thermomagnetization, field dependence of magnetization and the time dependent decay of remanent magetization were recorded using a SQUID magnetometer (Quantum design). The specific heat measurements in the temperature range 300–2 K were performed under ZFC condition in the PPMS and the data were collected during the warming cycle.

The reported metal to insulator transition (MIT) temperature ($T_{MI}$) is the temperature corresponding to the maximum in the electrical resistivity. The Curie temperature ($T_c$) and the spin freezing temperature ($T_g$) are denoted as the temperature corresponding to the high temperature maximum and low temperature maximum in the in-phase component of static bias field ac susceptibility respectively. The temperature at which $M_{ZFC}(T)$ and $M_{FC}(T)$ for a given magnetic field ($H$) start to bifurcate is represented as the temperature of irreversibility ($T_{irr}$).

## 3 Results and discussion

High statistics room temperature powder XRD patterns of bulk polycrystalline $La_{0.67}Ca_{0.33}Mn_{1-x}Ta_xO_3$ ($0 \leqslant x \leqslant 0.10$) compounds could be indexed to orthorhombic Pnma space group (Space group No. 62) [25]. The Rietveld refinement yielded an excellent agreement between the observed ($I_{obs}$) and calculated ($I_{cal}$) diffraction profiles with no peaks left un-indexed confirming the fact that the compounds are single phase [22]. The more detailed analysis and discussion of the crystal structure is published elsewhere [22]. The lattice parameters ($a$, $b$ and $c$) and average Mn-O distance ($\langle d_{\mathrm{Mn-O}} \rangle$) show a systematic increase with Ta substitution, hence an overall expansion of the unit cell (v) is observed. On the other hand, average Mn-O-Mn bond angle ($\langle \mathrm{Mn-O-Mn} \rangle$) shows a considerable decrease in the entire range of substitution. Thermogravimetry studies show that the oxygen stoichiometry of all the compounds is close to the nominal composition of 3 and is expected not to influence the physical properties of the compounds [22].

The ionic radius (IR) of $Ta^{5+}$ for the co-ordination number six is 0.64 Å [20]. Taking the IR alone in to account, substitution of $Ta^{5+}$ at the Mn site is not expected to introduce much of unit cell and local structural modification. However, the observed unit cell expansion of the $Ta^{5+}$ substituted compounds is understood in terms of the increase in the average Mn radius ($\langle IR_{\mathrm{Mn}} \rangle$) caused by changes in the average Mn valence of Mn. In this context, two effects are expected on the partial replacement of Mn by Ta differing in its valence state in

order to preserve the charge neutrality: either a reduction from $Mn^{4+}$ to $Mn^{3+}$ retaining the oxygen stoichiometry or the presence of excess oxygen in the lattice. If the changes in the oxygen stoichiometry were the dominant mechanism, it is expected that pentavalent Ta substitution decreases the unit cell parameters [26]. On the contrary, increase in unit cell parameters is observed for the Ta substituted compound. Furthermore, Rietveld analysis of the XRD patterns clearly established that pentavalent Ta substitution results in an increase of relative $Mn^{3+}$ concentration of the compounds. Thus, it is believed that the first mechanism is operative in the present case. Taking charge neutrality into account, $Ta^{5+}$ strongly shift the average valence state of Mn towards 3+ according to $La^{3+}_{0.67}Ca^{3+}_{0.33}Mn^{3+}_{(0.67+x)}Mn^{4+}_{(0.33-2x)}Ta^{5+}_{x}O^{2-}_{3}$. It is important to note that $Ta^{5+}$ not only increases the relative $Mn^{3+}$ concentration but also decreases the relative $Mn^{4+}$ concentration. A close agreement is seen between relative $Mn^{3+}$ and $Mn^{4+}$ concentration estimated from the refinement program and the one predicted based on the charge neutrality consideration [22]. Thus, shift of an average valence state of Mn ion to 3+ is expected to bring out an increase in the average Mn ionic radius ($\langle IR_{\mathrm{Mn}}\rangle$) and an associated increase in the lattice parameters.

The compounds with $x \leqslant 0.03$ exhibit a metal to insulator transition at $T_{MI}$ and close to it, a para to ferromagnetic transition at $T_c$ is also observed [25]. Beyond $x = 0.03$, the compounds exhibit an insulating behaviour with no perceptible anomaly near $T_c$, indicating the non-metallic behaviour of the ferromagnetic phase. It is worth mentioning that the reduction in $T_c$ as well as $T_{MI}$ is about ∼39 K/at.%, the larger extent reported for the Mn site substitutions in CMR manganites. While $T_{MI}$ decreases at a constant rate of ∼36 K/at.%, a linear decrease of similar rate (∼39 K/at.% is observed for $T_c$ up to $x = 0.03$, which levels off to a much smaller rate (∼10 K/at.% for higher Ta concentration. Under an application of magnetic field of 7 T, the compounds with $x \leqslant 0.03$ exhibit a significant reduction of $\rho$ with a shift of $T_{MI}$ to higher temperatures, a distinct feature of CMR manganites [25]. For $x > 0.03$, no field driven metallic state could be discerned at low temperatures even at a presence of 7 T [25]. Another striking feature of $x \geqslant 0.05$ is the presence of a cusp like feature in $\chi'(T)$ below $T_c$, followed by a broader shoulder at lower temperatures [25]. These results indicate that the Ta substitution modifies the ground state to a *glassy insulator*. For further understanding of the modified magnetic ground state of these compounds, we have carried out a detailed investigation of the static and dynamic magnetic responses of compounds with $x \geqslant 0.05$.

In the following, the static and dynamic responses, magnetic after effect and the spin energetic associated with the magnetic transition of the $La_{0.67}Ca_{0.33}Mn_{0.90}Ta_{0.10}O_3$ compound are discussed in detail. Figure 1 shows the dc susceptibility ($\chi_{dc}(T)$) as a function of the applied magnetic field ($H = 10$ Oe, 100 Oe and 1 kOe) for $x = 0.10$ in both ZFC and FC conditions. A broad cusp-like anomaly is found at a temperature just

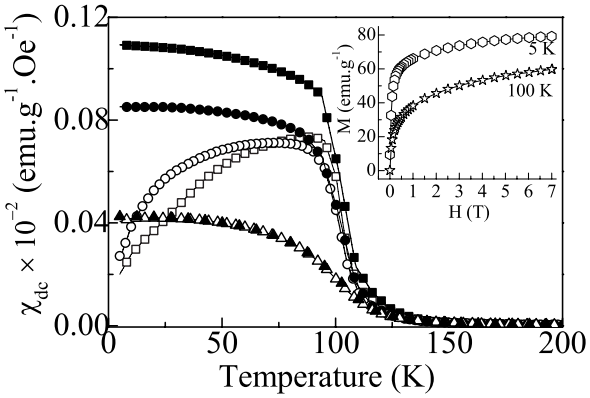


**Fig. 1.** ZFC (open symbols) and FC (closed symbols) thermomagnetization curves of $La_{0.67}Ca_{0.33}Mn_{0.90}Ta_{0.10}O_3$ compound for $H = 10$ Oe (□, ■), 100 Oe (○, ●), and 1 kOe (△, ▲). Inset shows the field dependence of magnetization at 100 K (☆) and 5 K (○).

below $T_c$ in ZFC $\chi_{dc}(T)$ when the applied field is 10 Oe, but this cusp loses its sharpness and becomes a broad maximum with an increasing magnetic field up to 1 kOe. An important point to be noted here is that the values of FC measurement of $\chi_{dc}(T)$ continue to increase strongly below the irreversibility temperature $T_{irr}$ (just below $T_c$), a typical feature of various cluster glass systems [27–29]. On the other hand in canonical spin glass systems, the FC $\chi_{dc}(T)$ shows a nearly constant value below $T_{irr}$ [30–33]. It is noteworthy that due to the fact that cluster-glass exhibit short range intra-cluster ferromagnetism below $T_c$, it may mimic some features of those found in re-entrant spin glass system (RSG). Nevertheless, it may be noted that in several RSG systems, $T_{irr} \ll T_c$ [34–37] whereas in a cluster glass, the irreversibility arises just below $T_c$ [38], as observed in Figure 1 for $x = 0.10$. Additionally, a strong reduction of the thermomagnetic irreversibility with enhancing measuring field indicates a field induced short range of inter-cluster ferromagnetic ordering below $T_{irr}$. The absence of long range ordering is also apparent from the non saturation of magnetization even up to a field of 7 T even at 5 K (inset of Fig. 1).

In order to probe the dynamics of spin freezing, $\chi'(T)$ was measured as a function of frequency ($\chi'(T, f)$) and static bias field ($\chi'(T, H)$). In the absence of static bias field, $\chi'(T, f)$ shows a frequency dependent cusp just below $T_c$ (Fig. 2a) and a broad shoulder at lower temperatures (marked by arrows in Fig. 2a). Since the ferromagnetic transition smears out the low temperature glass transition, it is difficult to identify the spin freezing temperature. At this point, it is important to note that the out of phase component, $\chi''$ (absorption part) of ac susceptibility does show characteristic maxima corresponding to the cusp-like anomaly and the shoulder feature in the $\chi'(T)$ curves. As a typical case, $\chi''(T)$ at $f = 10$ kHz is shown in the inset of Figure 2a. But the $\chi''$ signal became weak at lower temperature overwhelmed by noise especially for the lower excitation frequencies of $h$ and not much analysis could be carried out. Thus, the

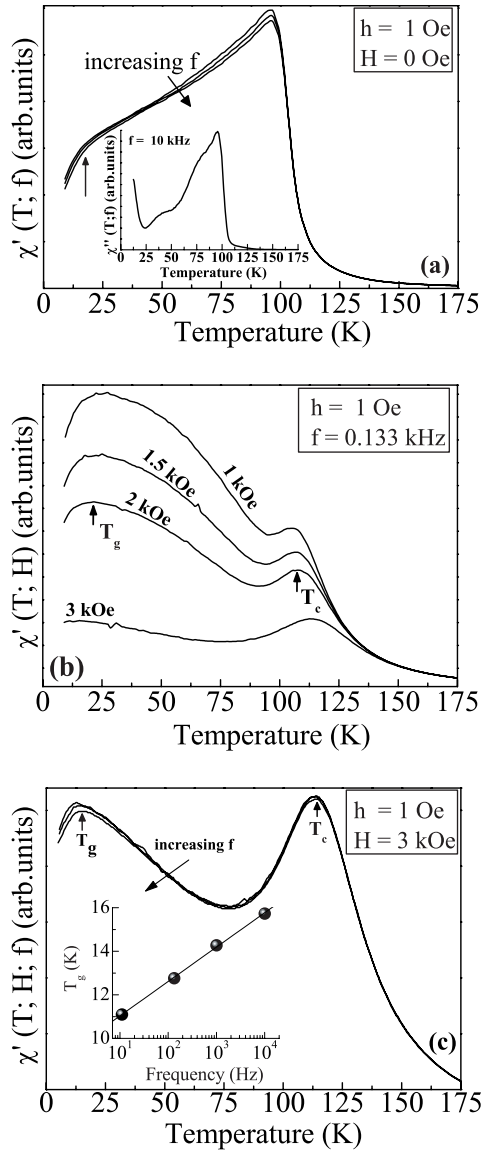


**Fig. 2.** Temperature variation of ac susceptibility of $La_{0.67}Ca_{0.33}Mn_{0.90}Ta_{0.10}O_3$ compound measured in (a) different frequencies ($f$) and in an ac field ($h$) of 1 Oe (b) different static bias fields with $f = 133$ Hz and $h = 1$ Oe (c) different $f$ and $h = 1$ Oe in 3 kOe static magnetic field. Inset of Figure 2a shows the temperature dependence of the out of phase component of ac susceptibility ($\chi''(T; f)$) for $f = 10$ kHz with $h$ of 1 Oe and inset of Figure 2c shows the frequency dependence of the freezing temperature ($T_g$) of the compound.

discussion of the dynamic response of the system is regrettably limited to the in-phase component $\chi'$ (dispersion part) of the ac susceptibility. The dynamic magnetic response gets modified drastically with an application of superimposed dc magnetic field (Fig. 2b). The suppression of $\chi'(T, H)$ and the broadening of the transition are due to the absence of long range ferromagnetic order as well as the slow response of the clusters in the presence of a static field. When the field is further increased, two distinct magnetic transitions, marking the ferromagnetic transition at $T_c$, followed by a spin freezing transition at $T_g(H)$ were found. With increasing magnetic fields, the decline of $\chi'(T, H)$ below 12 K and the shift of $T_g(H)$ to lower temperatures together confirm the presence of frozen spin disordered state. The shift in the susceptibility peak is not distinct in the absence of static bias field, whereas it is clearly seen at $T_g$(H) with an increase in frequency (133 Hz $\leqslant f \leqslant$ 10 kHz) in the presence of 3 kOe field (inset of Fig. 2c). The frequency dependent shift of $T_g(H)$ to higher temperature is one of the distinct features of cluster glass. It is worth mentioning that there is no frequency dependent shift of the peak at $T_c$. Moreover, the static and dynamic responses of the substituted compounds with $x = 0.05$ and 0.07 are also qualitatively similar to that of $x = 0.10$.

In the following, the qualitative features in the ac susceptibility that distinguish the CG, SG and super paramagnetic (SP) system are discussed. The SG [39–41] and SP system [42,43] show only a cusp in the ac susceptibility. The additional features, viz., a broad shoulder and /or a sharp drop of $\chi'$ signal at lower temperatures not only excludes the SG and SP state but also suggests the CG state of the compounds. The dynamic response of the RSG also mimics the CG systems. In the canonical spin glass systems, the cusp itself shows a frequency dependent shift to higher temperatures [39,40]. In CG, (Fig. 2c in the present case) as well as in the RSG, the position of cusp-like anomaly is frequency independent. The cusp-like anomaly in $\chi'$ and the shallow maximum in the ZFC static response of the system are close to each other and are entirely associated with clusters themselves and, but not with the SG system, or with the freezing of the magnetic moments. Moreover, in both RSG and CG, the cusp-like anomaly evolves into two distinct maxima under suitable static bias field: close to $T_c$ and at lower temperatures ($T_g$), marking the spin freezing temperature and a decline of $\chi'$ below this temperature. Unlike the high temperature maximum, the latter low temperature maximum in $\chi'$ signal exhibits a frequency dependent shift to higher temperatures, one of the characteristic features of both RSG and CG systems. However, based on the inter-comparison of the static response of the system under ZFC and FC conditions, it is argued that compounds with $x \geqslant 0.05$ of the present investigation show a CG rather than a RSG state.

Non-equilibrium spin dynamics is another characteristic feature of the cluster glass. The decay of remanent magnetization ($M(t)$) was measured in the temperature range 5–90 K (Fig. 3). A best fit using logarithmic relaxation of the functional form $M(t) = M_0[1 - S\ln(1 + t/t_0)]$ (where $M_0$ is the initial remanent magnetization, $S$ is the magnetic viscosity that depends on the magnetic field, temperature and material, $t_0$ is a reference time which depends on the sample and measuring procedure) is observed not only below but also above $T_g(H)$. The clear maximum of $S(T)$ close to $T_g(H)$ (inset of Fig. 3) results from the competition between two processes (i) freezing of magnetic moments due to the presence of competitive magnetic interactions (ii) activation of the frozen-in moments

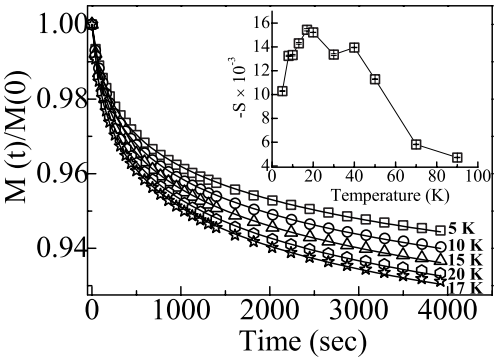


**Fig. 3.** Decay of remanent magnetization as a function of time of $La_{0.67}Ca_{0.33}Mn_{0.90}Ta_{0.10}O_3$ compound at selected temperatures. Straight line is the best fit to the experimental data. Inset shows magnetic visocity (S) as a function of temperature. Refer to text for details.

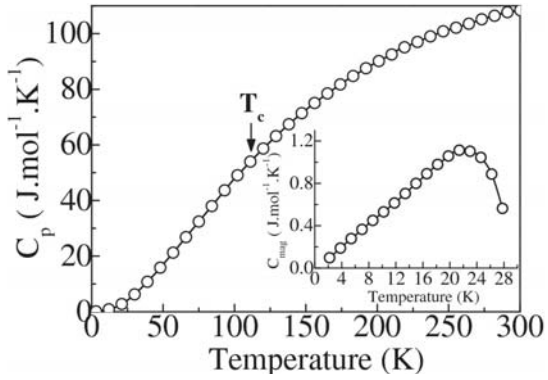


**Fig. 4.** Temperature dependence of specific heat ($C_p$) of $La_{0.67}Ca_{0.33}Mn_{0.90}Ta_{0.10}O_3$ compound. Inset shows the magnetic contribution to the total specific heat after subtracting the lattice contribution. Refer to text for details.

with increasing temperature. To ascertain the cluster glass state at zero field, specific heat measurements ($C_p(T)$) were carried out in the temperature range 2–300 K. No distinct anomaly corresponding to $T_c$ could be found in $C_p(T)$ (Fig. 4). In order to estimate the magnetic specific heat, the low temperature specific heat (2–25 K) is fitted by the following equation $C_p(T) = \beta T^3 + \alpha T^5 + \delta T^n$, where $\beta T^3 + \alpha T^5$ represents the lattice contribution and $\delta T^n$ is the spin wave contribution ($C_{mag}$) to the specific heat. The value of the exponent $n$ depends on the nature of the excitations. Since the compound is highly insulating, there is no electronic contribution to the total specific heat. The Debye temperature ($\theta_D$) is estimated to be $447 \pm 5.89$ K and is comparable with the reported values for manganites in the literature [44]. The value of n is estimated to be $1.04 \pm 0.01$, which is close to the glassy linear specific heat. The magnetic specific heat ($C_{mag}$) (inset of Fig. 4) is obtained after subtracting the phonon contribution. A linear temperature dependence of $C_{mag}$ together with a broad maximum just above $T_g$ provide an additional strong evidence for the cluster-glass state.

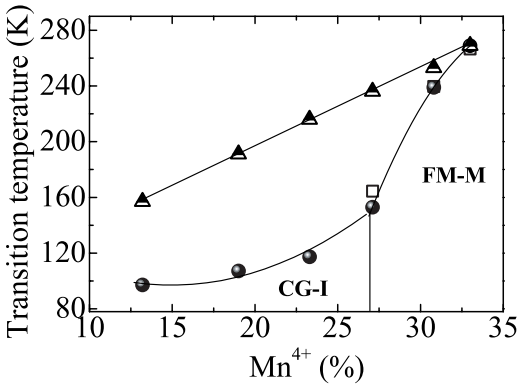


**Fig. 5.** Phase diagram of $La_{0.67}Ca_{0.33}Mn_{1-x}Ta_xO_3$ ($0 \leqslant x \leqslant 0.10$) compounds as a function of relative concentration of $Mn^{4+}$ (%) observed. FM-M and CG-I denote ferromagnetic-metal and cluster glass-insulator state respectively of the substituted compounds. For an inter comparison, similar plot for $La_{1-z}Ca_zMnO_3$ compounds (▲) (reproduced from S.-W. Cheong et al., *Colossal magnetoresistive oxides*, Monographs in Condensed Matter Science, edited by Y. Tokura (Gordon and Breach, London, 2000)) with same $Mn^{4+}$ concentration as that of substituted compounds are also given. Solid line is only guide to eye.

The microscopic consequences of $Ta^{5+}$ substitution are discussed in the following. It is apparent from the Rietveld studies that pentavalent Ta strongly shifts the average valence state of Mn towards 3+ to preserve the charge neutrality. Thus, the appreciable increase of the lattice parameters with $Ta^{5+}$ substitution can be understood as a result of the larger average ionic radius at the Mn site, though electron-lattice coupling might give an additional influence. Further, there is a substantial drop of the carrier density (relative $Mn^{4+}$ concentration) with increasing $x$ [25]. Indeed, the consequences of these two effects (reduced carrier density and increased ionic radius at the Mn site) should be displayed in a similar way by compounds $La_{1-z}Ca_zMnO_3$ [45,46], if the same level of doping ($Mn^{4+}$ content) is compared. For an inter-comparison, such curves are displayed in Figure 5. It is seen that the Ta substituted samples exhibit much lower values of $T_c$. For instance for $x = 0.05$, 23.1% of Mn sites contain $Mn^{4+}$ ions, leading to $T_c = 117$ K and low temperature glassy behaviour. On the other hand, ferromagnetism and metallicity are found in $La_{0.77}Ca_{0.23}MnO_3$ ($T_c \sim 220$ K) with the same doping level [46]. Therefore, the effects of carrier density and ionic size seem insufficient to account for the observed strong suppression of ferromagnetism. Larger structural modification involving an increase in $\langle d_{Mn-O} \rangle$ and a substantial decrease in $\langle Mn - O - Mn \rangle$ has been detected for Ta substituted compounds which is expected to decrease the DE interaction strength. The diamagnetic $Ta^{5+}$ ion ($4d^{10}$), by virtue of its closed shell configuration, just dilutes the magnetic network, and dilution generally results in a reduced magnetic ordering temperature. However, the degree of dilution is rather low in the studied compounds, and other diamagnetic substitutions for Mn

affect $T_c$ much less than Ta [16–18,47–49]. Hence, another microscopic effect seems necessary to understand the experimental result. As pointed out by Alonso et al. [50], the changes in charge state at the Mn site may create a random local electrostatic potential that attracts or repels charge carriers (holes). Taking the local electrostatic potential into account, calculations of these authors (carried out for $Ga^{3+}$ ions) indicate enhanced suppression of $T_c$ and glassy states. Due to the large positive charge of $Ta^{5+}$ ion, one would expect a strong electrostatic effect for this substitution, though the potential is positive in the case of $Ta^{5+}$. We suggest that this mechanism might contribute to the observed unusually strong suppression of the itinerant DE ferromagnetism. In the presence of antiferromagnetic super-exchange interactions and spatial disorder, the appearance of glassy behaviour is not unusual in manganites. The ability of $Ta^{5+}$ ion to induce cluster glass and insulating behaviour at very low Ta concentration ($x \sim 0.05$) if compared to other trivalent and tetravalent substitutions for Mn underlines the significance of charge state of the substituent in modifying the ferromagnetic-metallic ground state of CMR manganites.

At this point, the following remarks are being made. There are a few interesting works in recent time that addresses the issue of the glassy phase of manganites [51–53]. These studies have attempted to re-analyse the glassy phase of the compounds in the phase separation scenario. Recent theoretical works predict the co-existence of clusters in various length scales [54] below certain temperature $T^*$ and the only theoretical framework with similar characteristics is the phase separation scenario involving phases with different electron densities [55]. In the phase separation scenario, it is very likely that the quenched disorder and the competing exchange interactions among the clusters lead to the appearance of locally metastable states. The phase separated state (PSS), although does not constitute a conventional spin glass or cluster glass, share many of its features such as time or frequency dependent phenomena, that made to quote PSS as a *spin-glass like* or *cluster-glass like* state. This issue of phase separated glassy phase of manganites is currently under discussion and many more interesting results are expected in the near future. It is expected that the results presented in this paper will attain considerable attention for the theoretical frame work of the phase separated glassy state of manganite compounds.

## 4 Conclusion

Pentavalent Ta forms solid solution in the entire range of substitution and has left the crystal symmetry and the oxygen stoichiometry of the compounds unaltered. The observed unit cell expansion and the enhanced local structural modification with substitution is understood in terms of the increase in the average Mn radius due to Ta substitution. This study demonstrates that pentavalent substitution not only reduce the transition temperatures to the larger extent reported for the Mn site substituted manganites, but also induce a glassy behaviour at very low concentration ($x \sim 0.05$) compared to that of other divalent, trivalent or tetravalent substitutions for Mn in the ferromagnetic-metallic $La_{0.67}Ca_{0.33}MnO_3$. Besides modification of majority carrier concentration due to the increased $Mn^{3+}$ concentration and enhanced local structural effects, the local electro static potential due to the deviating charge state of the substituent at the Mn site seems to be certainly important and accounts for the unusually strong reduction in the itinerant ferromagnetism of the compounds. Static and dynamic responses of the compounds with $x \geqslant 0.05$ provide a strong indication that the modified magnetic ground state is a cluster-glass like state. Since the issue of a phase segregated state with glassy characteristics in the ferromagnetic-insulating phase is unresolved, the exact mechanism of the cluster-glass state of the compound remains open. Further studies are necessary in this direction.

Support by DFG, FOR520 is gratefully acknowledged. LSL also thanks CSIR, India for a Senor Research Fellowship.

## References

1. E. Dagotto, T. Hotta, A. Moreao, Phys. Reports **344**, 1 (2001) and references therein
2. A. Moreo, M. Mayor, A. Feiguin, S. Yunoki, E. Dagotto, Phys. Rev. Lett. **84**, 5568 (2002)
3. M. Uehara, S. Mori, C.H. Chen, S.-W. Cheong, Nature **399**, 560 (1999)
4. M. Fäth, S. Freisem, A.A. Menovsky, Y. Tomioka, J. Aarts, J.A. Mydosh, Science **285**, 1540 (1999)
5. J. Burgy, M. Mayor, V. Martin-Mayor, A. Moreo, E. Dagotto, Phys. Rev. Lett. **87**, 277202 (2001)
6. J. Burgy, A. Moreo, E. Dagotto, Phys. Rev. Lett. **92**, 097202 (2004)
7. E. Dagotto, New. J. Phys. **7**, 67 (2005)
8. P. Schiffer, A.P. Ramirez, W. Bao, S.-W. Cheong, Phys. Rev. Lett. **75**, 3336 (1995)
9. H.Y. Hwang, S.-W. Cheong, P.G. Radaelli, M. Marezio, B. Batlogg, Phy. Rev. Lett. **75**, 914 (1995)
10. P.G. Radaelli, G. Iannone, M. Marezio, H.Y. Hwang, S.-W. Cheong, J.D. Jorgensen, D.N. Argyriou, Phys. Rev. B **56**, 8265 (1997)
11. L.M. Rodriguez-Martínez, J.P. Attfield, Phys. Rev. B **63**, 024424 (2000)
12. A.J. Williams, B.M. Sobotka, J.P. Attfield, J. Solid State Chem. **173**, 456 (2003)
13. J.P. Attfield, Crystal Eng. **5**, 427 (2002)
14. K.H. Ahn, X.W. Wu, K. Liu, C.L. Chien, Phys. Rev. B **54**, 15299 (1996)
15. M. Rubinstein, D.J. Gillespie, J.E. Snyder, T.M. Tritt, Phys. Rev B **56**, 5412 (1997)
16. V.P. S. Awana, E. Schmitt, E. Gmelin, A. Gupta, A.V. Narlikar, O.F. De Lima, C.A. Cardoso, S.K. Malik, W.B. Yelon, J. Appl. Phys. **87**, 5034 (2000)
17. J. Blasco, J. Garcia, J.M. de Teressa, M.R. Ibarra, J. Perez, P.A. Algarabel, C. Marquina, Phys. Rev. B **55**, 8905 (1997)
18. X. Liu, X. Xu, Y. Zhang, Phys. Rev. B **62**, 15112 (2000)
19. L. Seetha Lakshmi, V. Sridharan, D.V. Natarajan, V.S. Sastry, T.S. Radhakrishnan, J. Phys. Pramana **58**, 1019 (2001)

20. R.D. Shannon, C.T. Prewitt, Acta. Crystallogr. Sec. A. **32**, 751(1976)
21. L. Seetha Lakshmi, K. Dörr, K. Nenkov, A. Handstein, K.-H. Müller, V.S. Sastry, J. Phys: Condens. Matter. **19**, 216218 (2007)
22. L. Seetha Lakshmi, K. Dörr, K. Nenkov, V.S. Sastry, K.-H. Müller, J. Phys: Condens. Matter. **19**, 236207 (2007)
23. A.C. Larson, R.B. von Dreele, Los Alamos National Laboratory Report LAUR (2000) pp. 86–748
24. M.W. Lufaso, P.M. Woodward, Acta Cryst. B **57**, 725 (2001)
25. L. Seetha Lakshmi, K. Dörr, K. Nenkov, V. Sridharan, V.S. Sastry, K.-H. Müller, J. Magn. Magn. Mater. **290-291**, 924 (2005)
26. L. Malavasi, M.C. Mozzati, C.B. Azzoni, G. Chiodelli, G. Flor, Solid State Commun. **123**, 321 (2002)
27. Y. Sun, X. Xu, wei Tong, Y. Zhang, Appl. Phys. Lett. **77**, 2734 (2000)
28. Z.-H. Wang, B.-G. Shen, N. Tang, J.-W. Cai, T.-H. Ji, G.-C. Che, S. -Y Dai, Dickon, H.L. Ng, J. Appl. Phys, **85**, 5399 (1999)
29. R.-w. Li, Z.-h. Wang, X. Chen, J.-R. Sun, B-G. Shen, C.-H. Yan, J. Appl. Phys. **87**, 5597 (2000)
30. R. von Helmolt, L. Haupt, K. Bärner, U. Sondermann, Solid State Commun. **82**, 693 (1992)
31. L. Haupt, R. Von Helmolt, U. Sondermann, K. Bärner, Y. Tang, E.R. Giessinger, E. Ladizinsky, R. Braunstein, Phys. Lett. A **165**, 473 (1992)
32. M. Itoh, I. Natori, S. Kubota, K. Motoya, J. Phys. Soc. Jpn. **63**, 1486 (1994)
33. Y. Moritomo, Y. Tomioka, A. Asamitsu, Y. Tokura, Y. Matsui, Phys. Rev. B **51**, 3297 (1995)
34. W. Abdul-Razzaq, J.S. Kouvel, H. Claus, Phys. Rev. B **30**, 6480 (1984)
35. W. Abdul-Razzaq, J.S. Kouvel, Phys. Rev. B **35**, 1764 (1987)
36. T. Ando, E. Ohta, T. Sato, J. Magn. Magn. Mater. **163**, 277 (1996)
37. S.N. Kaul, S. Srikanth, J. Phys.: Condens. Matter. **10**, 11067 (1998)
38. S. Mukherjee, R. Ranganathan, P.S. Anilkumar, P.A. Joy, Phys. Rev. B **54**, 9267 (1996)
39. K. Binder, A.P. Young, Rev. Mod. Phys. **58**, 801 (1986)
40. J.A. Mydosh, *Spin glasses; An experimental introduction* (Taylor & Francis, London, 1993)
41. C.A. M. Mulder, A.J. van Duyneveldt, J.A. Mydosh, Phys. Rev. B **23**, 1384 (1981)
42. J.L. Dormann, R. Cherkaoui, L. Spinu, M. Noguès, F. Lucari, F. D'. Orazio, D. Fiorani, A. Garcia, E. Tronc, J.P. Jolivet, J. Magn. Magn. Mater. **187**, L139 (1998)
43. C.S. Lue, J.H. Ross Jr, K.D. D. Rathnayaka, D.G. Naugle, S.Y. Wu, W.-H. Li, J. Phys.: Condens. Matter. **13**, 1585 (2001)
44. L. Ghivelder, I. Abrego Castillo, N. McN Alford, G.J. Tomka, P.C. Riedi, J. MacManus-Driscoll, A.K. M. Akther Hossain, L.F. Cohen, J. Magn. Magn. Mater. **189**, 274 (1998)
45. P. Schiffer, A.P. Rameriz, W. Bao, S.-W. Cheong, Phys. Rev. Lett. **75**, 3336 (1995)
46. S.-W. Cheong, H.Y. Hwang in *Colossal Magnetoresistive Oxides*, edited by C.N. R. Rao, Y. Tokura (Gordon and Breach Science Publishers, India, 2000), p. 237
47. Y. Sun, X. Xu, L. Zheng, Y. Zhang, Phys. Rev B **60**, 12317 (1999)
48. M.C. Sanchez, J. Blasco, J. García, J. Stankiewicz, J.M. de Teressa, M.R. Ibarra, J. Solid State Chem. **138**, 226 (1998)
49. J.R. Sun, G.H. Rao, B.G. Shen, H.K. Wong, Appl. Phys. Lett. **73**, 2998 (1998)
50. J.L. Alonso, L.A. Fernández, F. Guinea, V. Laliena, V. Martín-Mayor, Phys. Rev. B **66**, 104430 (2002)
51. F. Rivadulla, M.A. López-Quintela, J. Rivas, Phys. Rev. Lett. **93**, 167206 (2004)
52. J. Rivas, F. Rivadulla, M.A. López-Quintela, Physica B **354**, 1 (2004)
53. F. Rivadulla, J. Rivas, J.B. Goodenough, Phys. Rev. B **70**, 172410 (2004)
54. A. Moreo, M. Mayr, A. Feiguin, S. Yunoki, E. Dagotto, Phys. Rev. Lett. **84**, 5568 (2000)
55. A. Moreo, S. Yunoki, E. Dagotto, Science **283**, 2034 (1999)